

# ENVIRONMENTAL RESEARCH FOOD SYSTEMS



## LETTER

### OPEN ACCESS

#### RECEIVED

10 November 2025

#### REVISED

9 March 2026

#### ACCEPTED FOR PUBLICATION

7 May 2026

#### PUBLISHED

2 June 2026

Original content from this work may be used under the terms of the [Creative Commons Attribution 4.0 licence](#).

Any further distribution of this work must maintain attribution to the author(s) and the title of the work, journal citation and DOI.



## Mapping global cereal flows at subnational scales uncovers heterogeneities in sourcing dependencies

Shruti Jain\*

Smith School of Enterprise and the Environment, University of Oxford, Oxford, United Kingdom  
Institute of Environmental Sciences (CML), Leiden University, Leiden, The Netherlands

\* Author to whom any correspondence should be addressed.

E-mail: [s.jain@cml.leidenuniv.nl](mailto:s.jain@cml.leidenuniv.nl)

**Keywords:** global food flows, subnational, food systems resilience

Supplementary material for this article is available [online](#)

### Abstract

Subnational data on both domestic and international cereal flows is essential for understanding food supply chain vulnerabilities, yet no such dataset exists at a global scale. This study estimates spatially resolved cereal flow networks across 3540 subnational regions in 195 countries using a triply-constrained spatial interaction model that simultaneously enforces regional supply-demand balance and consistency with reported bilateral trade statistics. Domestic distribution accounts for approximately 25% of global cereal consumption, and 17% is met through international trade. Nearly half of net importing countries contain surplus regions that supply grain domestically, while virtually every net exporting country retains deficit regions reliant on inflows. Crop-disaggregated supply profiles reveal that subnational regions with similar aggregate trade dependency can have fundamentally different supply structures, differing in which crops dominate their consumption, whether those crops are sourced locally, domestically, or internationally, and how concentrated their sources are. Source concentration over exporting countries varies across subnational regions and across crops, revealing vulnerability hotspots that national-level assessments cannot detect. These subnational, crop-specific flow estimates can support targeted policy interventions to reduce supply chain vulnerabilities and enable more spatially precise environmental footprinting of food supply chains.

## 1. Introduction

Agricultural trade has more than doubled between 1995 and 2018 [1], accounting for 19% of globally consumed calories [2], which has allowed the flow of food from regions with surplus to those with deficit [3, 4]. Trade can serve as an adaptation mechanism under climate change [5], and as resources like land and water become limited with climate change, the role of trade in distributing food will become even more important. At the same time, these distribution networks can further geopolitical, environmental, and climate related vulnerabilities in the form of food production, export restrictions, and transport disruptions [6, 7]. With regional specialization, major breadbaskets have become sole suppliers of agricultural commodities to other nations [8], and such structural food dependence of food deficit countries can be disadvantageous, if food surplus countries decide to impose international trade restrictions [9]. Overall, the potential of trade to enhance food security can only be realized if the associated risks of increased exposure to external stresses are understood and mitigated [10].

Extensive research has characterized food trade networks at the national level, documenting increasing connectivity [11–13] and growing trade dependency [14, 15]. Yet the balance between the benefits of trade connectivity and the risks of import exposure plays out at subnational scales and national analyses mask critical variation [16]—a country can appear food-secure in aggregate while specific regions face acute deficit and differentiated risk exposure [17]. Moreover, existing analyses focus almost exclusively on international trade, yet domestic redistribution remains largely unquantified at a global

scale [16]. Studies of subnational flows exist for individual countries [18–20], but no dataset provides a globally consistent picture of both domestic and international flows at subnational resolution. This limits not only food security analysis but also the environmental footprinting of food supply chains, since production conditions vary enormously within countries and tracing impacts to specific consuming regions requires subnational, crop-specific flow data [18, 21–23].

This study addresses these gaps by estimating cereal flows between all first-level administrative regions in 195 countries, covering both domestic and international distribution for wheat, rice, maize, other cereals. A spatially-constrained gravity model is used to estimate cereal flows, an approach well-suited to this problem because it allocates cereals from surplus to deficit regions across a global network while respecting known bilateral trade volumes, producing realistically diversified flow patterns without requiring subnational trade data that does not exist for most countries. These ‘flows’ explicitly link the region of production with the final destination of import, and hence provide an accurate estimate of regional import dependencies. This work focuses on cereal grains given that they form the most important source of calories for a majority of the world’s population, either directly or indirectly via animal feed [24]. The estimated flows are used to: (i) quantify the scale and geography of domestic cereal redistribution relative to international trade; (ii) reveal subnational heterogeneities in trade dependency and self-sufficiency that are invisible at national scales; and (iii) assess how supply composition, sourcing, and concentration differ across regions and cereal crops. These results provide a foundation for more spatially precise environmental footprinting of food supply chains and for targeted interventions to reduce supply chain vulnerabilities. Throughout, ‘self-sufficiency’ is used for the share of consumption met by local production, ‘trade dependency’ for the share met by inflows, and ‘concentration’ for the degree to which supply is dominated by few partners, measured by the Herfindahl–Hirschman index (HHI).

## 2. Methods

This study estimates the flow of cereals between 3540 subnational regions in 195 countries by downscaling available data on the bilateral flow of cereals at national scales. The modelling pipeline comprises three main components: (i) pre-processing the production and bilateral trade data from the FAO and other sources, (ii) estimating subnational flows using a triply-constrained spatial interaction model, i.e. a gravity model that simultaneously enforces origin supply, destination demand, and bilateral trade constraints, and (iii) validating the estimates against independent empirical data.

### 2.1. Data inputs

The primary data inputs are FAO’s national-scale statistics on the production, distribution, and consumption for 15 cereal commodities—barley, buckwheat, canary seed, fonio, maize, millet, mixed grain, oats, quinoa, rice, rye, sorghum, triticale, wheat, other—for the years 2017–2021. This 5 year window was the most recent period with complete reporting for all countries at the time of this analysis. Although this interval includes the COVID-19 pandemic, it remains representative of typical global cereal flows, as global cereal trade volumes were not significantly disrupted by the pandemic [25]. The five-year average further smooths any transient disruption.

Discrepancies between the volume of cereal trade reported by importing and exporting countries were resolved using a reliability index approach [26] (supplementary methods 1). A re-export algorithm [22] was then applied to obtain cereal ‘flows’ that link the source of production with the destination of import and ensure that total exports from a country never exceed its production and imports combined (supplementary methods 2). The resulting flows represent total cereal movements including for food, feed, and other uses. These processing steps were implemented separately for each crop and year, then aggregated across cereal commodities and averaged over 2017–2021.

Subnational production was derived from the MapSPAM global gridded crop production dataset [27], aggregated to administrative boundaries and scaled to match FAO national production totals for 2017–2021. Subnational consumption was estimated via a log-linear gamma regression fitted at the national scale, using livestock counts, population, GDP, and cereal production as predictors (supplementary methods 3). The fitted model was applied at subnational scales and the resulting estimates scaled so that within each country their sum matches the FAO-reported national consumption total. Transport costs between all pairs of subnational regions were obtained from Verschuur *et al* [28], who estimated the cost (USD/tonne) of transporting grain commodities between subnational regions globally (supplementary table 1).

## 2.2. Triply-constrained spatial interaction model

This study employs a triply-constrained spatial interaction model based on entropy-maximization principles [29, 30] to estimate subnational cereal flows. This approach generates the most probable distribution of flows across a network, given known constraints on regional supply, regional demand, and bilateral trade volumes. It simultaneously routes domestic and international flows within a unified global matrix, using transport costs as the spatial friction. The flow of a given cereal crop  $X_{ij}$  from subnational region  $i$  to region  $j$  is modelled as:

$$X_{ij} = A_i \cdot B_j \cdot K_{AB} \cdot S_i \cdot D_j \cdot Tr_{ij}^{-\beta}$$

where  $S_i$  is the tradable surplus in origin region  $i$ , defined as  $\max(P_i - C_i, 0)$ ;  $D_j$  is the deficit demand in destination region  $j$ , defined as  $\max(C_j - P_j, 0)$ ;  $Tr_{ij}$  is the transport cost between regions;  $\beta$  is the transport cost elasticity of trade, set to 1.5;  $A_i$  and  $B_j$  are regional balancing factors; and  $K_{AB}$  is a country-pair balancing factor where  $i \in \text{Country A}$  and  $j \in \text{Country B}$ . The balancing factors are solved iteratively to ensure that the origin, destination, and bilateral trade constraints are satisfied. The value of  $\beta$  reflects the expectation that trade in bulk agricultural commodities decays more steeply with transport cost than the distance elasticities of approximately 1.0 typically estimated for aggregate trade [31]; sensitivity analysis confirmed that results are robust across  $\beta = 1.2$ – $1.8$ .

The model enforces three mass-balance constraints: (i) the sum of outflows from each region equals its tradable surplus, (ii) the sum of inflows to each region equals its deficit, and (iii) the sum of all subnational flows between any two countries matches the observed FAO bilateral trade volume. The third constraint implicitly captures non-distance trade frictions—including tariffs, geopolitical alignments, and trade agreements—without requiring their explicit parameterization. Domestic trade targets are set as the residual surplus after accounting for international exports. The model is solved via iterative proportional fitting [32], with convergence defined as the maximum absolute error across all constraints falling below 1 tonne (supplementary methods 4). The model is run independently for four crop categories: wheat, rice, maize, and other remaining cereals. This gravity model framework is readily generalizable to other commodity groups given appropriate production, consumption, and bilateral trade data.

## 2.3. Sensitivity analysis

To test the sensitivity of estimated flows to the assumed cost elasticity  $\beta$ , the baseline network ( $\beta = 1.5$ ) was compared against two perturbed models ( $\beta = 1.2$  and  $\beta = 1.8$ ). The resulting network structure proved highly robust in both cases. For all crops, the rank-order of all trade corridors remained nearly identical (Spearman's  $\rho \geq 0.99$ ), the models shared a common part of flows (CPF)  $\geq 0.96$  with the baseline, and flow volumes were highly correlated ( $R^2 \geq 0.99$ ). Over 98% of the highest-volume trade routes (the top 5th percentile) remained consistent across scenarios (supplementary table 4).

## 2.4. Validation

The model was validated against two independent datasets. First, modelled US domestic cereal flows were compared against the Freight Analysis Framework version 5 (FAF5) for 2017–2021. Validation here focuses on comparing aggregate regional outflows and inflows, because the transshipment problem makes direct link-level comparison structurally ambiguous: the same grain may travel through intermediate logistics hubs in freight surveys but appear as a direct origin-to-destination flow in the gravity model (supplementary methods 4). Modelled cereal flows and US FAF flows showed strong rank correlation for regional outflows ( $\rho = 0.70$ ,  $p < 0.01$ ). Inflow correlation was weaker ( $\rho = 0.26$ ,  $p \approx 0.07$ ), but this is because FAF data identifies major port states, such as Louisiana and Washington, as top domestic destinations, whereas the gravity model clears international demand directly from producing regions.

The model was also validated against Indian interstate cereal flows estimated by Harris *et al* [18] for 2012. Despite a decade-long temporal gap, the model achieved strong nodal correlations for both outflows ( $\rho = 0.77$ ,  $p < 0.01$ ) and inflows ( $\rho = 0.74$ ,  $p < 0.01$ ). Agreement was strongest for wheat and weakest for maize. At the link level, the aggregate cereal network achieved  $\rho = 0.42$  ( $p < 0.01$ ) and CPF = 0.45, indicating that the model correctly identified the spatial pathways for nearly half of India's physical grain volume. Wheat showed the strongest crop-specific alignment, capturing the centralized outward flow from India's northwest breadbaskets. Rice, maize, and other cereals showed substantially weaker alignment, consistent with the heavy intervention of India's Public Distribution System in rice routing [18] and the structural shift of Indian maize from human consumption to feed over the intervening decade [33]. Note that the Harris *et al* [18] estimates include internationally sourced cereals within their interstate flow estimates, whereas our model separates domestic and international flows explicitly, some divergence between the two is therefore expected. Full validation metrics by crop are reported in supplementary table 5.

### 3. Results

#### 3.1. The scale of domestic and international distribution

International flows of cereals sum up to about 455 million tonnes and account for 16.6% of global production, and global domestic flows make up a total of about 691 million tonnes which is 25.1% of global production. Approximately 1610 million tonnes (~58% of global production) are consumed within the regions where they are produced. Domestic redistribution thus exceeds international trade by a factor of 1.6, which underscores the critical role of internal distribution networks in global food supply.

Both national and subnational flows follow a heavily right-skewed distribution: most flows are small, with a few very large flows dominating total volumes. At the subnational level, flows can be separated into two types: those that cross international borders and those that move within countries. The within-country flows are substantially larger—the biggest domestic corridors carry roughly seven times the volume of the biggest international ones (supplementary table 6). The largest within-country corridors connect breadbaskets to major consumption centres: Nebraska to Texas (5.8 Mt), Iowa to California (5.1 Mt), and Heilongjiang to Guangdong (5.0 Mt). By contrast, the largest cross-border subnational corridors are smaller and connect neighbouring countries, dominated by flows from France and Argentina (supplementary table 6). Aggregating across all trading partners, the regions with the largest total outflows are Heilongjiang (China), Iowa (United States), and Henan (China) for within-country flows, and Córdoba (Argentina), Mato Grosso (Brazil), and Saskatchewan (Canada) for cross-border flows. The largest inflow destinations are Guangdong (China), Texas (United States), and Sichuan (China)—these are populous, industrialized regions that depend on distant breadbaskets within their own countries (supplementary table 7). The volume of within-country flows is strongly correlated with national population ( $r = 0.79$ ), reflecting the role of internal distribution in routing production from geographically concentrated production zones to dispersed consumption centres.

Figure 1 illustrates these patterns. Panel (a) shows the national-scale flows derived from FAOSTAT. The width of the links indicates the volume of trade flows, and the colour indicates the exporting region. Panel (b) shows the top 5% of the cereal flows at subnational scales, revealing a denser, more geographically distributed network in which domestic flows within India, China, Indonesia, and the United States are visually prominent, a pattern that is entirely absent from the national-scale map. Notably, the international flow corridors visible at national scales fragment into many smaller subnational links, while the domestic flows that are invisible at national scales emerge as some of the largest individual corridors in the network. Panel (c) shows the domestic flow of cereals in 6 select countries—Spain, Colombia, Ethiopia, United States, New Zealand, and India—illustrating how internal redistribution patterns vary from highly centralized (Ethiopia and New Zealand) to more distributed (India and the United States).

#### 3.2. Subnational heterogeneity within countries

Nearly half of all net importing countries contain surplus regions with net outflows, while virtually every net exporting country retains deficit regions dependent on inflows. In net importing countries, several breadbasket regions generate substantial internal surpluses (figure 2(a)). Heilongjiang, Henan, and Jilin in China ship significant cereal volumes southward. Spain's Castilla y León, Indonesia's Sumatera Selatan, and Mexico's Sinaloa likewise supply domestic shortfalls. In sub-Saharan Africa, Ethiopia's Oromia, Nigeria's Kebbi, and South Africa's Free State function as net internal exporters. However, very little of these surpluses reaches international markets (figure 2(b)), suggesting that breadbasket regions in net importing countries are primarily serving a domestic buffering function.

The mirror pattern holds in net exporting countries. Within the United States, Texas, California, and North Carolina depend on domestic heartlands for their cereal supply. In India, Jharkhand, Maharashtra, Bihar, and Gujarat rely on the Northwestern breadbasket, and Brazil's São Paulo and Bahia depend on their national production centres (figure 2(c)). International imports into deficit regions of net exporting countries are generally modest but significant in a few cases, including Brazil and Germany (figure 2(d)). These patterns suggest that subnational flow data is needed to accurately assess regional food security, since a country's aggregate trade position alone provides limited insight into its individual regions.

#### 3.3. Self-sufficiency and trade dependence

Figure 3 quantifies, for each subnational region, the share of cereal consumption met by domestic inflows versus international inflows. Regions in Latin America, the Middle East, and North Africa are disproportionately reliant on international inflows, with many meeting most of their cereal demand through imports. In Asia, large producers such as India, China, and Indonesia are predominantly self-sufficient through domestic distribution, while regions in Japan and South Korea rely heavily on

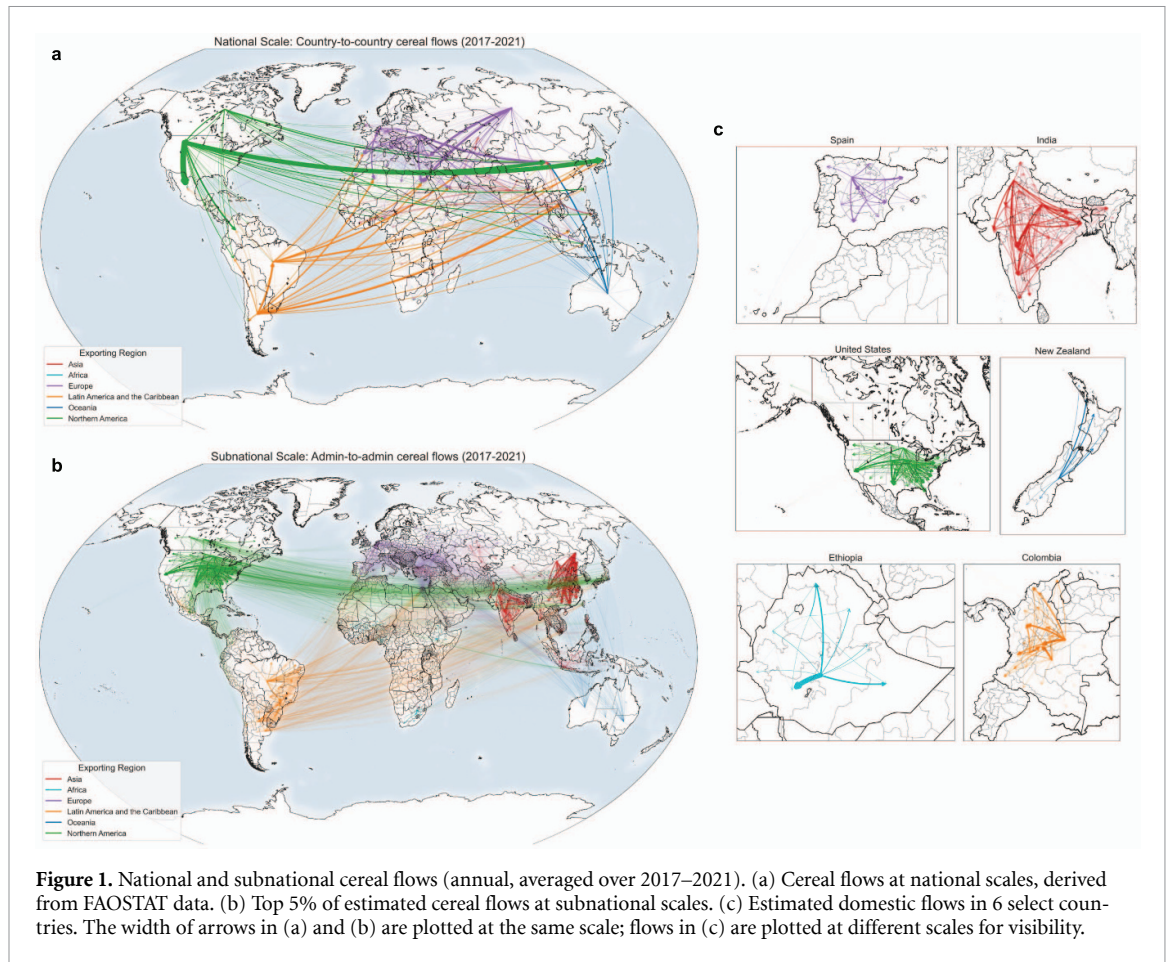


**Figure 1.** National and subnational cereal flows (annual, averaged over 2017–2021). (a) Cereal flows at national scales, derived from FAOSTAT data. (b) Top 5% of estimated cereal flows at subnational scales. (c) Estimated domestic flows in 6 select countries. The width of arrows in (a) and (b) are plotted at the same scale; flows in (c) are plotted at different scales for visibility.

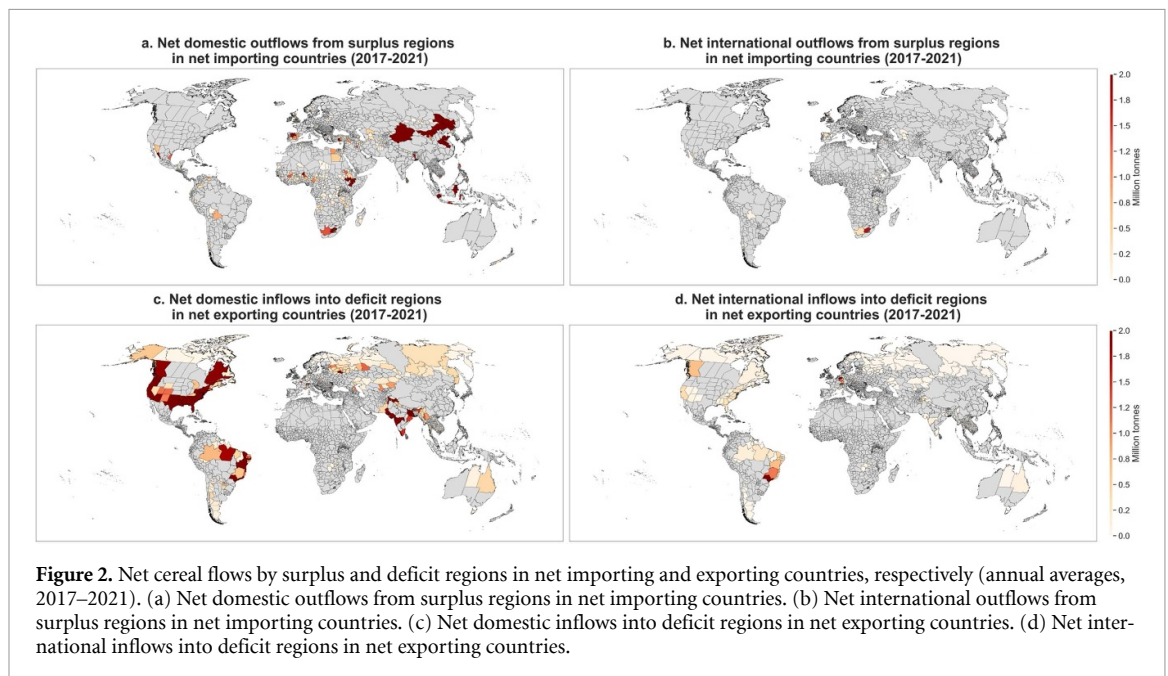
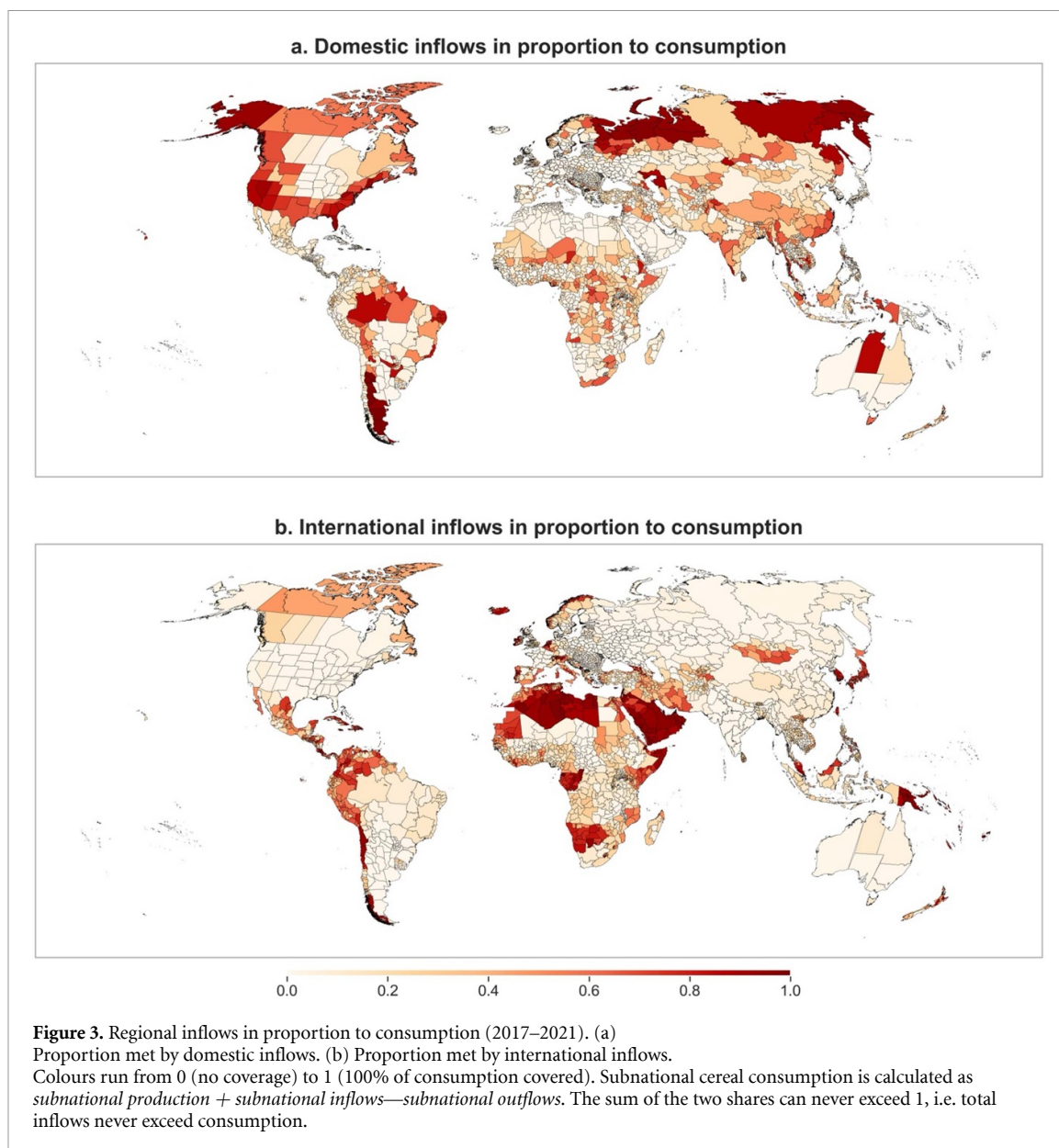


**Figure 2.** Net cereal flows by surplus and deficit regions in net importing and exporting countries, respectively (annual averages, 2017–2021). (a) Net domestic outflows from surplus regions in net importing countries. (b) Net international outflows from surplus regions in net importing countries. (c) Net domestic inflows into deficit regions in net exporting countries. (d) Net international inflows into deficit regions in net exporting countries.

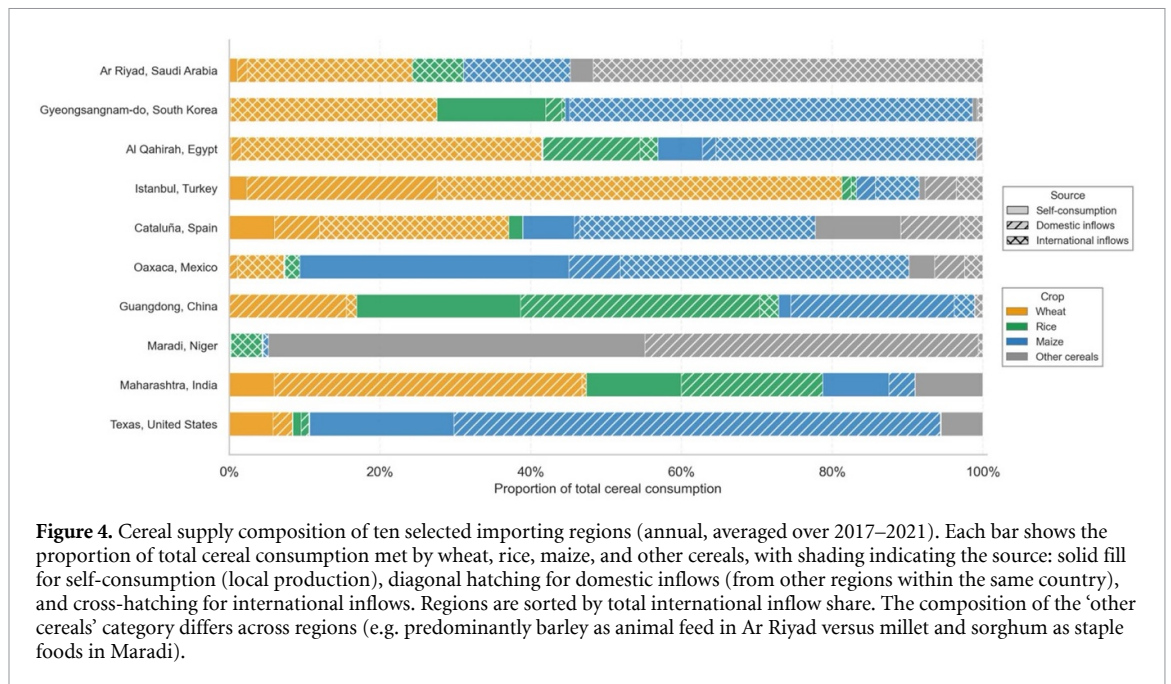
international inflows. North American and Russian regions are similarly dominated by domestic redistribution. European regions are the most mixed, with many drawing substantially on both domestic and international sources. A continental breakdown (supplementary figure 2) shows that domestic flows contribute most to consumption in Northern America and least in Africa, while international inflows are most prominent in Africa and Latin America. Majority of the international inflows into Africa, Asia, and



Latin America and the Caribbean, originate from outside the continent. On the other hand, most international inflows into Europe come from within the continent, which can be attributed to the common market and agricultural policy of the European Union. A comparison of international inflows, outflows, and within-country flows for the 20 countries with the largest cereal flows is shown in supplementary figure 3.

### 3.4. Crop-specific supply profiles

The aggregate patterns in figure 3 treat cereals as a single commodity and cannot reveal whether a region's supply is dominated by one crop or spread across several, nor whether different crops follow the same sourcing channels. To examine this, cereal flows were disaggregated by crop (wheat, rice, maize, and other cereals) and the supply composition of ten importing regions spanning diverse geographies and dependency profiles was characterized (figure 4). The crop composition and sourcing of cereal supply vary across regions, such that regions with similar aggregate trade dependency can have fundamentally different vulnerability profiles. Ar Riyad (Saudi Arabia) and Gyeongsangnam-do (South Korea) are both heavily dependent on international cereal inflows (95% and 82% respectively), yet their profiles are very different. Ar Riyad's dependency spans all crop categories, whereas Gyeongsangnam-do meets most of its rice demand from domestic production and depends on international sources only for wheat and maize. A disruption to global wheat markets would severely affect Gyeongsangnam-do's cereal supply but leave its rice supply intact, whereas Ar Riyad would be affected across the board.



At the other end of the spectrum, Texas (United States) and Maharashtra (India) are both predominantly domestically supplied but through very different crop channels. In Texas, self-produced and domestically sourced maize from the US corn belt constitutes the majority of cereal consumption, reflecting large-scale livestock feed demand. Maharashtra draws on wheat from northern Indian states and rice from southern states. A drought in India’s northern breadbasket would disrupt Maharashtra’s wheat supply while leaving its rice and maize channels intact, whereas Texas’s vulnerability is concentrated in a single crop system. Other regions illustrate further diversity. Guangdong (China) draws substantially on wheat, rice, and maize through both domestic and international sources. Maradi (Niger) depends almost entirely on other cereals, sourced from local production and domestic inflows, making it vulnerable to production shocks affecting the wider region. Al Qahirah (Egypt) shows heavy international wheat and maize dependency alongside substantial domestic rice inflows. Cataluña (Spain) shows a mix of domestic production and international sourcing across multiple crops, wheat primarily from within the EU, maize primarily from Latin America.

These supply profiles demonstrate that aggregate measures of trade dependency systematically understate crop-specific vulnerabilities. To quantify this further, the HHI<sup>1</sup> was used to assess concentration in crop-specific flow networks. The HHI measures the relative size of firms within an industry and serves as an indicator of market competitiveness—it was shown to be empirically linked to food price-volatility risk at the national level by Karakoc and Konar [34]. High international dependency does not necessarily imply high source concentration. Gyeongsangnam-do imports about 99% of its wheat and maize internationally yet maintains HHI values below 0.25 for both, indicating effective supplier diversification. Ar Riyad similarly shows low wheat HHI (0.15) but high rice HHI (0.63), revealing uneven diversification across crops. Conversely, moderate international dependency can mask acute single-source risk. Oaxaca’s international maize imports account for 47% of consumption but come almost entirely from one country, the United States (HHI = 0.91). Istanbul’s wheat imports, at 66% of wheat consumption, show an HHI of 0.54, indicating reliance on two dominant suppliers (Russia and Ukraine). supplementary figure 4 maps the HHI of international cereal inflows at subnational resolution for each crop, restricted to regions where the crop constitutes at least 20% of cereal consumption and more than 20% is sourced internationally. The crop-specific maps highlight which regions within a country face concentrated supply risk and for which cereals. These examples demonstrate that assessing supply chain vulnerability requires examining both the level of international dependency and its concentration across source countries, at the level of individual crops and individual regions—a resolution that only subnational, crop-disaggregated flow data can provide.

<sup>1</sup> This index ranges from 0 to 1, with 0 representing a highly competitive market and 1 indicating a monopoly. An HHI < 0.15 indicates a competitive market, and HHI between 0.15 and 0.25 indicates moderate concentration, and an HHI > 0.25 indicates high levels of market concentration.

## 4. Discussion and conclusions

This study provides the first globally consistent estimate of cereal flows at subnational resolution, covering both domestic and international distribution for wheat, rice, maize, and other cereals across 3540 administrative regions. Three principal findings emerge.

First, domestic redistribution constitutes the largest component of global cereal distribution, yet has been almost entirely absent from global food trade analyses. Domestic flows exceed international flows on every continent except Africa. Harris *et al* [18] and Karakoc *et al* [20] documented substantial domestic cereal redistribution in India and the United States respectively; our results place these individual-country findings in a global context, extending global trade analyses such as D'odorico *et al* [11] to include the domestic dimension that most studies omit. Second, the subnational heterogeneity within countries, with surplus and deficit regions coexisting regardless of aggregate national trade position, demonstrates that national-level indicators mask critical spatial variation. Domestic redistribution can partially buffer international supply shocks, and the surplus regions identified within net importing countries may play a critical role in this regard. Third, the crop-disaggregated analysis reveals that aggregate measures of trade dependency systematically understate vulnerability. Regions with similar aggregate import shares can have fundamentally different risk profiles depending on which crops they import, from where, and with what source concentration. These findings extend Kummu *et al* [14] documentation of declining partner diversity and Hernández *et al* [35] analysis of rising agrifood concentration to the subnational and crop-specific level.

The gravity model framework could be extended to incorporate additional commodity groups, time-series analysis to track evolving dependencies, and integration with climate scenarios to simulate the impact of production shocks on subnational supply chains. These flow estimates also provide a foundation for more accurate environmental footprinting of food supply chains. By linking specific consuming regions to their actual production sources, subnational flows enable the attribution of production-side environmental impacts—greenhouse gas emissions, water use, fertilizer application, land use change—to the regions that drive demand for those products.

Several limitations should be noted. The gravity model assumes transport cost is the primary spatial friction, and while the bilateral trade constraint implicitly captures tariffs, geopolitical alignments, and institutional relationships, factors such as government procurement systems and pre-existing contracts are not explicitly modelled—likely explaining the weaker validation performance for rice and maize in India. Regional consumption is computed separately rather than endogenously, which may over- or under-estimate the tradeable surplus in regions. Gridded crop production data may contain spatial misallocations that propagate into flow estimates. Furthermore, the modelled flows represent total cereal movements including feed and industrial uses, and should be interpreted accordingly. Finally, out-of-sample validation was possible only for the United States and India, and as subnational validation data becomes available for more countries, confidence in the estimates can be further strengthened.

The identification of concentrated supply corridors, crop-specific dependencies, and highly import-dependent regions provides a spatial evidence base for targeted interventions, such as storage infrastructure placement, transport corridor investment, and crop-specific diversification strategies. These findings can support policies aligned with the United Nations' SDG 2 (Zero Hunger) and SDG 13 (Climate Action), while also informing regional initiatives such as EU's Common Agricultural Policy and the Comprehensive Africa Agriculture Development Programme [36–38].

## Acknowledgments

This research was made possible through funding support from Oxford Reuben Interdisciplinary Scholarship in Environmental Change, awarded by Reuben College at the University of Oxford. Thank you to the three anonymous reviewers whose feedback immensely improved this article. SJ would also like to thank Samuel Fankhauser, Michael Clark, and Jasper Verschuur, for offering their valuable feedback on this manuscript.

## Data availability statement

The data that supports the findings of this study are openly available in the supplementary files of this article.

Supplementary information available at <https://doi.org/10.1088/2976-601X/ae69e9/data1>.

Subnational boundaries available at <https://doi.org/10.1088/2976-601X/ae69e9/data2>.

Subnational cereal flows available at <https://doi.org/10.1088/2976-601X/ae69e9/data3>.

## Code availability

The code needed to analyze the data and reproduce the figures from this study is publicly available in this [GitHub repository](#).

## Conflict of interest

Authors declare that they have no competing interests.

## ORCID iD

Shruti Jain  [0000-0002-8697-2673](https://orcid.org/0000-0002-8697-2673)

## References

- [1] FAO 2022 *The State of Agricultural Commodity Markets 2022. The Geography of Food and Agricultural Trade: Policy Approaches for Sustainable Development* (FAO) (<https://doi.org/10.4060/cc0471en>)
- [2] Martin W and Laborde Debuquet D 2018 Trade: the free flow of goods and food security and nutrition *IFPRI Book Chapters* (International Food Policy Research Institute (IFPRI)) pp 20–29
- [3] Suweis S, Carr J A, Maritan A, Rinaldo A and D’Oro P 2015 Resilience and reactivity of global food security *Proc. Natl Acad. Sci.* **112** 6902–7
- [4] Janssens C, Havlik P, Boere E, Palazzo A, Mosnier A, Leclère D, Balkovič J and Maertens M 2022 A sustainable future for Africa through continental free trade and agricultural development *Nat. Food* **3** 608–18
- [5] Janssens C *et al* 2020 Global hunger and climate change adaptation through international trade *Nat. Clim. Change* **10** 829–35
- [6] Wellesley L, Preston F, Lehne J and Bailey R 2017 Chokepoints in global food trade: assessing the risk *Res. Transp. Bus. Manage.* **25** 15–28
- [7] Centeno M A, Nag M, Patterson T S, Shaver A and Windawi A J 2015 The emergence of global systemic risk *Annu. Rev. Sociol.* **41** 65–85
- [8] Puma M J, Bose S, Chon S Y and Cook B I 2015 Assessing the evolving fragility of the global food system *Environ. Res. Lett.* **10** 024007
- [9] Paillard S, Dorin B, Le Cotty T, Ronzon T and Treyer S 2011 Food security by 2050: insights from the agrimonde project *European Foresight Platform Brief* 196
- [10] Brown M E, Carr E R, Grace K L, Wiebe K, Funk C C, Attavanich W, Backlund P and Buja L 2017 Do markets and trade help or hurt the global food system adapt to climate change? *Food Policy* **68** 154–9
- [11] D’odorico P, Carr J A, Laio F, Ridolfi L and Vandoni S 2014 Feeding humanity through global food trade *Earth’s Future* **2** 458–69
- [12] Sartori M and Schiavo S 2015 Connected we stand: a network perspective on trade and global food security *Food Policy* **57** 114–27
- [13] Zhang Y-T and Zhou W-X 2022 Structural evolution of international crop trade networks *Front. Phys.* **10** 926764
- [14] Kummu M, Kinnunen P, Lehtikoinen E, Porkka M, Queiroz C, Rösös E, Troell M and Weil C 2020 Interplay of trade and food system resilience: gains on supply diversity over time at the cost of trade independency *Glob. Food Secur.* **24** 100360
- [15] Porkka M, Kummu M, Siebert S, Varis O and Hart J P 2013 From food insufficiency towards trade dependency: a historical analysis of global food availability *PLoS One* **8** e82714
- [16] Porkka M, Guillaume J H, Siebert S, Schaphoff S and Kummu M 2017 The use of food imports to overcome local limits to growth *Earth’s Future* **5** 393–407
- [17] Stokeld E, Croft S A, Green J M and West C D 2020 Climate change, crops and commodity traders: subnational trade analysis highlights differentiated risk exposure *Clim. Change* **162** 175–92
- [18] Harris F, Dalin C, Cuevas S, Nr L, Adhya T, Joy E J, Scheelbeek P F, Kayatz B, Nicholas O and Shankar B 2020 Trading water: virtual water flows through interstate cereal trade in India *Environ. Res. Lett.* **15** 125005
- [19] Pandit A, Karakoc D B and Konar M 2023 Spatially detailed agricultural and food trade between China and the United States *Environ. Res. Lett.* **18** 084031
- [20] Karakoc D B, Wang J and Konar M 2022 Food flows between counties in the United States from 2007 to 2017 *Environ. Res. Lett.* **17** 034035
- [21] Li M, Jia N, Lenzen M, Malik A, Wei L, Jin Y and Raubenheimer D 2022 Global food-miles account for nearly 20% of total food-systems emissions *Nat. Food* **3** 445–53
- [22] Croft S A, West C D and Green J M 2018 Capturing the heterogeneity of sub-national production in global trade flows *J. Cleaner Prod.* **203** 1106–18
- [23] Liu W, Antonelli M, Kummu M, Zhao X, Wu P, Liu J, Zhuo L and Yang H 2019 Savings and losses of global water resources in food-related virtual water trade *Wiley Interdiscip. Rev.* **6** e1320
- [24] Awika J M 2011 Major cereal grains production and use around the world *Advances in Cereal Science: Implications to Food Processing and Health Promotion* (ACS Publications) pp 1–13
- [25] Arita S, Grant J, Sydow S and Beckman J 2022 Has global agricultural trade been resilient under coronavirus (COVID-19)? Findings from an econometric assessment of 2020 *Food Policy* **107** 102204

- [26] Gehlhar M 1996 Reconciling bilateral trade data for use in GTAP *GTAP Technical Papers* (Global Trade Analysis Project (GTAP), Center for Global Trade Analysis, Department of Agricultural Economics, Purdue University, West Lafayette, IN.) pp 11
- [27] International Food Policy Research, I 2024 *Global Spatially-Disaggregated Crop Production Statistics Data for 2020 Version 2.0 Version V4* (Harvard Dataverse) (<https://doi.org/10.7910/DVN/SWPENT>)
- [28] Verschuur J, Vittis Y, Obersteiner M and Hall J W 2025 Heterogeneities in landed costs of traded grains and oilseeds contribute to unequal access to food *Nat. Food* **6** 36–46
- [29] Wilson A 2013 *Entropy in Urban and Regional Modelling (Routledge Revivals)* (Routledge)
- [30] Jaynes E T 1957 Information theory and statistical mechanics *Phys. Rev.* **106** 620
- [31] Head K and Mayer T 2014 Gravity equations: workhorse, toolkit, and cookbook *Handbook of International Economics* vol 4 (Elsevier) pp 131–95
- [32] Sinkhorn R 1967 Diagonal equivalence to matrices with prescribed row and column sums *Am. Math. Mon.* **74** 402–5
- [33] FAO 2023 *FAOSTAT*
- [34] Karakoc D B and Konar M 2024 Optimization of national grain imports to balance risk and return: a portfolio theory approach *Environ. Res.* **1** 011001
- [35] Hernández M A, Espinoza A, Berrospi M L, Deconinck K, Swinnen J and Vos R 2023 *The Role of Market Concentration in the Agrifood Industry* vol 2168 (Intl Food Policy Res Inst)
- [36] United Nations n.d. Sustainable development goals: 17 goals to transform our world (available at: [www.un.org/en/exhibits/page/sdgs-17-goals-transform-world](http://www.un.org/en/exhibits/page/sdgs-17-goals-transform-world)) (Accessed 1 October 2024)
- [37] European Commission n.d. *The common agricultural policy at a glance* (available at: [https://agriculture.ec.europa.eu/common-agricultural-policy/cap-overview/cap-glance\\_en](https://agriculture.ec.europa.eu/common-agricultural-policy/cap-overview/cap-glance_en)) (Accessed 1 October 2024)
- [38] African Union n.d. Comprehensive African Agricultural Development Programme (CAADP) (available at: <https://caadp.org/>) (Accessed 1 October 2024)